Gene expression profiles in normal and *Otx2*$^{-/-}$ early gastrulating mouse embryos

Lise Zakin*, Bruno Reversade*, Bérangère Virlon†, Christophe Rusniok‡, Philippe Glaser‡, Jean-Marc Elalouf†, and Philippe Brûlet*§

*Unité d'Embyologie Moléculaire, Unité de Recherche Associée 1947, Centre National de la Recherche Scientifique, and ‡Laboratoire de Génomique des Microorganismes Pathogènes, Institut Pasteur, 25 Rue du Docteur Roux, 75724, Paris Cedex 15, France; and †Département de Biologie Cellulaire et Moléculaire, Service de Biologie Cellulaire, Unité de Recherche Associée 1859, Centre National de la Recherche Scientifique, Centre d'Energie Atomique, Saclay, 91191 Gif-sur-Yvette Cedex, France

Communicated by François Jacob, Institut Pasteur, Paris, France, October 27, 2000 (received for review October 2, 2000)

The mouse *Otx2* gene is a homeobox transcription factor required as early as gastrulation for the proper development of the head. We compared gene expression profiles in wild-type and *Otx2*$^{-/-}$ 6.5 days postcoitum embryos by using a serial analysis of gene expression assay adapted to microdissected structures. Among a broader list, the study of six genes found to be differentially expressed allows defining a role for *Otx2* in the orchestration of cell movements leading to the adequate organization of the embryo before gastrulation.

Mutation of the *Drosophila orthodenticle* (*otd*) gene specifically affects the development of the most anterior segments of the fly fated to form the head (1). Numerous *Otd* homologues have been found in a variety of species covering most of the metazoan phyla, based on the conservation of a bicoïd class homeodomain (2). Two murine *Otd* homologues, *Otx1* and *Otx2*, were characterized and shown to be also associated with rostral development. The transcription factor *Otx2* is the first of these two genes to be expressed in the course of murine development [5.75 days postcoitum (dpc)]. Ubiquitously transcribed in the embryonic ectoderm and visceral endoderm before gastrulation, *Otx2* is progressively restricted from 6.5 to 7.5 dpc to the anterior region of the embryo as the primitive streaks elongates. Later, *Otx2* is transcribed in the cephalic region and the developing sense organs (3).

Functional studies revealed that *Otx2* is required as early as gastrulation for normal development of the brain. Thus, embryos homozygous for a targeted mutation of *Otx2* display an early lethal phenotype characterized by the lack of head structures anterior to rhombomere 3 (4). Further analysis by means of chimeric embryos demonstrated that *Otx2* expression is sequentially necessary, in the visceral endoderm at the onset of gastrulation for neural induction, and later in the anterior neuroectoderm itself, to specify forebrain and midbrain regions (4, 5). Understanding of the mechanisms involved in the acquisition of anterior identity requires the identification of *Otx2* downstream genes, among which should be the factor(s) that, in the visceral endoderm, mediate anterior neuroectoderm induction.

Large-scale analysis of gene expression should conceivably help in delineating such downstream genes. We therefore used the serial analysis of gene expression (SAGE) method, which provides quantitative gene expression profiles (6), and was recently scaled-down to make possible the analysis of microdissected structures (7). Two SAGE libraries were constructed, from wild-type (WT) and *Otx2*$^{-/-}$ embryos at early gastrulation (6.5 dpc), the stage at which *Otx2* function is primarily required. Then, 140 differentially represented mRNA tags were identified, and several mRNAs were further analyzed by *in situ* hybridization. Our study therefore allows the identification of several *Otx2* potential target genes and describes global anterior–posterior patterning defects in *Otx2*$^{-/-}$ embryos.

Table 1. Abundance values of tags corresponding to genes involved in embryogenesis

Tag	WT	Otx2$^{-/-}$	GenBank match
TCTAATGACT	1	1	Nodal gene, a TGF-β-like gene
AAAGCCAAGC	1	1	Lim1, putative transcription regulator
CAATTCCTGA	0	1	Cerberus-related 1 (Cerr1)
AGGCTGAGCT	**4**	**0**	**Embryonic ectoderm development protein (eed)**
CAGAGGCAGG	**0**	**2**	**Wnt-4**
TTCACTCTGG	1	0	Fibroblast growth factor receptor 1 (bFGF-R)
CTCTTGCCCC	1	0	Fibroblast growth factor 4 (FGF-4)
GTGCTGGAGA	1	2	Fibroblast growth factor 8 (FGF-8)
ATATTTATGT	**2**	**0**	**Fibroblast growth factor (FGF-15)**
CCATCTGGTG	3	0	Transforming growth factor α (TGFα)
TAATTGCTGT	2	0	Distal-less homeobox 1 (Dlx-1)
GATGCCGTGG	1	3	Gl/S-specific cyclin D3
TCCCTGAGTT	1	0	E-cadherin
TGGAGGTGGA	2	2	Smad3
AGAAAGATGC	1	1	Smad4

The sequence of the tag is given along with its abundance in the WT and *Otx2*$^{-/-}$ libraries, as well as the identity of the transcript from which it originates. Bold characters indicate that differential expression was confirmed by *in situ* hybridization.

Materials and Methods

Embryos Genotyping, *in Situ* Hybridization, and 5-Bromo-4-Chloro-3-Indolyl β-D-Galactoside (X-Gal) Staining. Embryos were obtained by mating *Otx2*$^{+/-}$ mice. Midday of the day of the vaginal plug was considered 0.5 dpc. Embryos were dissected at room temperature in PBS and processed for the generation of SAGE libraries or *in situ* hybridization and X-Gal staining. For SAGE libraries, the embryonic and extraembryonic portions were separately transferred into 1.5-ml polypropylene tubes. Each portion was centrifuged for 2 min at 2000 $\times$ *g*, frozen in liquid nitrogen, and stored at -80°C until use. Embryo genotyping was performed by PCR on the extraembryonic portion as previously described (4). X-Gal staining and whole-mount *in situ* hybridization of embryos were carried out as previously described by Acampora *et al.* (4) and Henrique *et al.* (8), respectively. Hybridization probes were generated from IMAGE

Abbreviations: *otd*, *orthodenticle*; dpc, days postcoitum; SAGE, serial analysis of gene expression; WT, wild type; EST, expressed sequence tag; AVE, anterior visceral endoderm; *Dkk-1*, *Dickkopf-1*.

§To whom reprint requests should be addressed. E-mail: pbrulet@pasteur.fr.

The publication costs of this article were defrayed in part by page charge payment. This article must therefore be hereby marked "*advertisement*" in accordance with 18 U.S.C. §1734 solely to indicate this fact.

Article published online before print: *Proc. Natl. Acad. Sci. USA*, 10.1073/pnas.011513398. Article and publication date are at www.pnas.org/cgi/doi/10.1073/pnas.011513398

Table 2. List of tags present at higher levels in the *Otx2*$^{-/-}$ than in the WT library

Tag	WT	KO	KO/WT	*P*	GenBank match
ATAAAAAAAA	0	9	>9	0.004	Peroxisomal PTS2 receptor (U69171)
TACGAGCACA	1	9	9.0	0.018	EST, highly similar to ubiquinol cytochrome C reductase (AA033187)
TTGCCTTATT	1	9	9.0	0.018	EST 331499, similar to human IP-30 protein (W13914)
TTCCCAGAAA	1	9	9.0	0.018	EST, similar to ATP synthase subunit D mitochondrial (D13120)
AGCGTGGCCT	0	8	>8	0.008	AAC-11 inhibitor of apoptosis (U35846)
AGCCCCGCCT	0	8	>8	0.008	Integrin binding protein kinase, ILK (U94479)
TCTCTAAATA	2	16	8.0	0.001	Cystatin B (U59807)
CGCTTGGCAG	1	8	8.0	0.030	Δ Proteasome subunit (U13393)
TTCTGTGCAG	1	8	8.0	0.030	EST J0515B06 (AU0119257)
TGACACCCTT	1	8	8.0	0.030	EST 633613 (AA184527)
TGTTCATACA	0	6	>6	0.018	ESTs (AI155073; AA433547)
TGTAGTCTGC	0	6	>6	0.018	EST, similar to human argine rich protein (AA217925)
CCCCTCCCAC	0	6	>6	0.018	ESTs (AA871006; AI115602; W64163)
TTCTATGCCT	3	19	6.3	0.001	EST 493579 (AA087133)
TCCTTTGCCC	0	5	>5	0.042	Zona pellucida (Zp-1) gene, exon 1 (U24227)
TGCTGAAGGA	0	5	>5	0.042	Zinc finger protein Requiem (req) (U10435)
TGGGGTAGAT	0	5	>5	0.042	Calregulin (ERp60) (M92988)
TGTGGGAAAA	0	5	>5	0.042	EST, vanin 3 (AI118382)
ATAGCAAAGA	0	5	>5	0.042	EST, similar to canis familiaris VIP-36 protein (AW229370)
AGCACAGCCT	0	5	>5	0.042	EST 947464 (AI505056)
AGTTTGCTCA	0	5	>5	0.042	Peroxisomal biogenesis factor (Pex11b) (AF093671)
CAGGCGGCCA	0	5	>5	0.042	Catenin α 1 (X59990)
GAGTACTTTT	0	5	>5	0.042	Purine-nucleoside phosphorylase (X56548)
CTGAATGACG	2	11	5.5	0.012	Nuclear RNA helicase Bat1 (AF118128)
GCAGAACCAG	3	16	5.3	0.003	A10 mRNA, partial cds (L21027)
CTGCTCCTGC	2	10	5.0	0.025	Metallothionein 2 (K02236)
AGTTTGTCTG	2	10	5.0	0.025	EST 1480726 (AI035276)
AGCGAAGTGG	2	10	5.0	0.025	EST, highly similar to human N-terminal acetyltransferase (AA068754)
CAACTCCAAT	2	9	4.5	0.049	Calpactin I light chain (p11) (M16465)
TTTTGCACAG	2	9	4.5	0.049	ESTs 765113; 947489 (J0528F02)
CTGAGAACTT	2	9	4.5	0.049	β-Globin gene (AA960070)
GGAATGCGGG	2	9	4.5	0.049	EST 1248132 (AA960070)
GTGACTGGGT	5	21	4.2	0.001	Mitochondrial cytochrome c oxidase subunit IV (COX IV) (M37829)
TTGTTGGAGG	3	11	3.7	0.033	EST (W29669)
TTAAATAAAA	3	11	3.7	0.033	Sid393p (AB025049)
GTGTTGTTTA	5	14	2.8	0.037	cdc2 mRNA for CDC2 kinase (X16461)
CTGTGTGTGG	7	18	2.6	0.033	Prostatic secretory glycoprotein (p12) (X06342)
TGAAAATTGG	9	23	2.6	0.015	COX7cl mRNA for cytochrome c oxidase VIIc (X52940)
GACAAGGCCA	28	67	2.4	0.000	Apolipoprotein A–I (X64262 S37)
ATTTCAAGAA	9	21	2.3	0.022	EST 1450276 (AI035675)
CACGTTGTCA	8	18	2.3	0.050	Embigin precursor (J03535)
AATAAACCGT	8	18	2.3	0.050	Adenine phosphoribosyltransferase (APRT) (M11310)
CAAAAAAAAA	11	24	2.2	0.025	EST 863707 (AA512428)
TGGGGAAAGG	13	28	2.2	0.021	Ribosomal protein L35a (Y16430)
TTTGCCGGCA	27	58	2.1	0.001	Ubiquitin (X51703)
AATAAAGTGG	16	33	2.1	0.016	Cyclophilin (M60456)
AATGCCCTCA	65	130	2.0	0.000	Acidic ribosomal phosphoprotein P1 (U29402)
GAGAGGGCAA	84	162	1.9	0.000	Ribosomal protein S12 (X15962)
TGAAATGAAC	23	44	1.9	0.010	EST 475993 (AA049909)
GTTCCAAAGC	24	45	1.9	0.011	Hexokinase 1 (J05277)
CGTATTACCT	27	49	1.8	0.010	REX-3 (AP051347)
CCGCGAGGCC	42	75	1.8	0.003	Ribosomal protein S26 (RPS26) (U67770)
TTCCAGGCCC	20	35	1.8	0.029	Apolipoprotein E (M12414)
AAAGCCCGGA	79	138	1.7	0.001	Ribosomal protein S8 (X73829)
GCATTGCCAA	62	107	1.7	0.001	J1 protein, yeast ribosomal protein L3 homologue (Y00225)
AGCAAGCAGG	45	77	1.7	0.003	Cytoplasmic beta-actin (MI2481)
CTCCTTGTCA	23	38	1.7	0.048	Phosphatidylethanolamine binding protein (U43206)
AGAAAAAAAA	36	57	1.6	0.027	Skeletal muscle chloride channel (X62897)
AAACAACCCA	37	56	1.5	0.045	Mitochondrial gene for cytochrome b (X57779)
AAGCGGGCTT	51	76	1.5	0.020	EST, highly similar to human ribosomal 60S protein L34 (AA574826)
GGGGTTTACC	76	110	1.4	0.012	Ribosomal protein S16 (M11408)
AATGATGAGG	79	105	1.3	0.040	Heat shock protein 70 cognate (M19141)

Each tag is given its sequence, its abundance in both libraries (WT and KO), the ratio value (KO/WT), the *P* value calculated by Monte–Carlo simulations, and its GenBank match. Only tags displaying GenBank matches are shown. The complete list of tags obtained in WT and *Otx2*$^{-/-}$ will be available at http://www.dsv.cea.fr/thema/get/sade.html.

Table 3. List of tags present at lower levels in the *Otx2*$^{-/-}$ than in the WT library

Tag	WT	KO	WT/KO	*P*	GenBank match
CTCCTGCCCC	9	0	>9	0.01	ClpP protease (AJ005253)
CTAGAGGAAA	9	1	9.0	0.03	EST 1005223 (AA606898)
ATGCCGCCCC	8	1	8.0	0.04	Nonmuscle tropomyosin 5 (X53753)
GTCGTGACAG	8	1	8.0	0.04	p68 RNA helicase (X65627)
TTCAATTTAA	8	1	8.0	0.04	ESTs (AI047965; AA967648)
CAACAAAGGT	7	0	>7	0.02	HSP60 protein (X53584)
ATAGTTGCTA	6	0	>6	0.03	EST 577496 (AA139307)
ACAGAGATGA	5	0	>5	0.05	ESTs, similar to human hypothetical protein (Q15004)
ACCATCCTGA	13	3	4.3	0.01	rbm3 (AB016424)
TCTTGTGAAA	12	3	4.0	0.02	EST 597651 (AI447986)
AGCTGAAGGT	21	6	3.5	0.01	Suil (Z50159)
ACCTTTGCAT	10	3	3.3	0.05	Protein arginine methyltransferase (Carm1) (AF117887)
AAGAAGCCAC	46	19	2.4	0.00	Pyrubate kinase M (D38379)
TGATTCCCTC	48	21	2.3	0.00	External transcribed spacer (X56974)
CACATCTCAA	50	24	2.1	0.00	24.6-kDa protein (M93980)
TTGTTACAGA	33	19	1.7	0.04	EST J1008D06 (AU041730)
TCTACCATTT	40	24	1.7	0.04	EST, highly similar to human 40S ribosomal protein (AI931810)
TCTCTTCCCA	90	56	1.6	0.01	Ribosomal protein S4 (Rps4) (M73436)
TGATGCCCTC	466	306	1.5	0.00	α-Galactosidase A (U34071)
TGACTCCCTC	1118	955	1.2	0.00	B2 repetitive sequence (M31447)
TGACGCCCTC	461	394	1.2	0.02	Pelle-like protein kinase (AF103876)

The content of each column is similar to that described in Table 2. Additional data will be available at http://www.dsv.cea.fr/thema/get/sade.html.

clones by *in vitro* transcription using digoxygenin-UTP for RNA labeling. Embryos genotypes were established by PCR after hybridization and staining.

Generation of SAGE Libraries. The embryonic portions of *Otx2*$^{+/+}$ or *Otx2*$^{-/-}$ embryos harvested at 6.5 dpc were used to generate SAGE libraries. Thirty embryos were used in each case. Libraries were generated by using the SAGE adaptation for downsized extracts (SADE) method (7). Poly(A) RNAs were isolated through hybridization to oligo(dT)$_{25}$ covalently bound to magnetic beads by using Dynabeads mRNA direct kit (Dynal, Great Neck, NY). Briefly, frozen embryos were pooled in 100 μl of lysis binding buffer supplemented with 2 μg glycogen (Roche Molecular Biochemicals). After extensive rinsing of the beads, first-strand cDNA was synthesized by using Superscript Moloney murine leukemia virus (M-MLV)

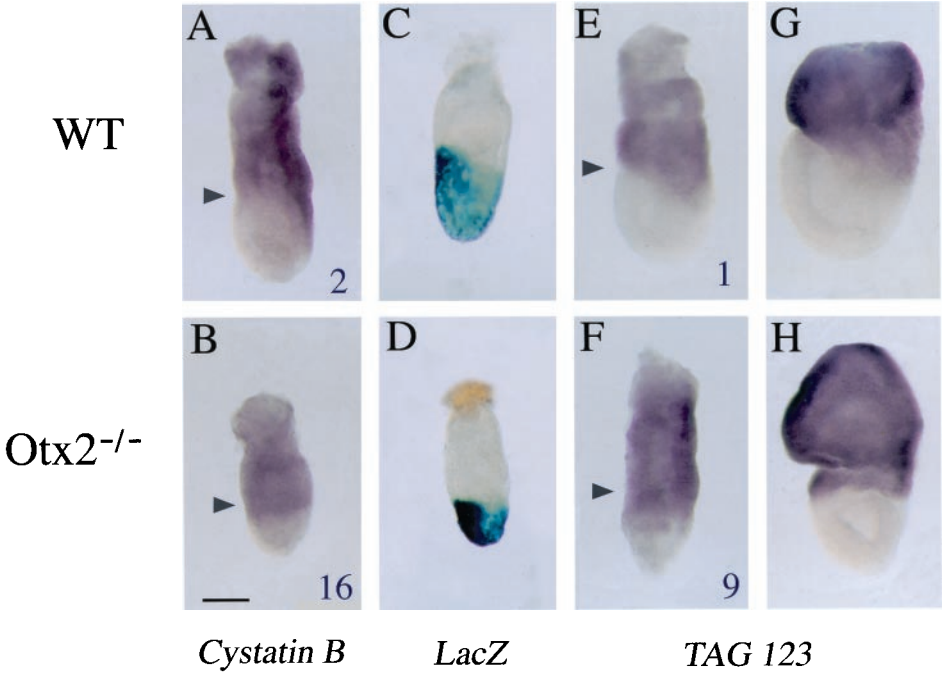

Fig. 1. Expression of mRNAs for *cystatin B* and tag 123 in WT and *Otx2*$^{-/-}$ embryos at 6.5 and 7.5 dpc, and comparison to the *Otx2* transcription domain. Values at the lower right hand corner of *A*, *B*, *E*, and *F* show tag abundance in the two libraries. The black arrowheads point to the embryonic–extraembryonic junction. (*A* and *E*) Expression of mRNAs for *cystatin B* and tag 123 in 6.5 dpc WT embryos. (*B* and *F*) Expression of mRNAs for *cystatin B* and tag 123 in 6.5 dpc *Otx2*$^{-/-}$ embryos. (*G* and *H*) Expression of mRNA for tag 123 in 7.5 dpc embryos. (*C* and *D*) β-galactosidase staining of *Otx2*$^{+/-}$ and *Otx2*$^{-/-}$ embryos carrying a *LacZ* reporter gene in the *Otx2* locus. (Scale bar: 100 μm.)

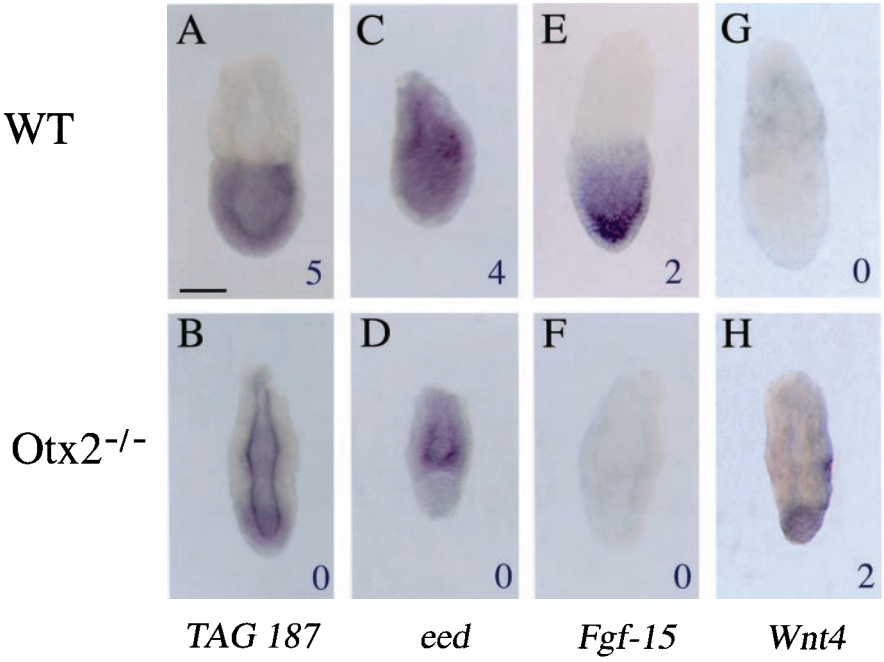

Fig. 2. Expression of mRNAs for tag 187 (Q15004), *eed*, *Fgf-15*, and *Wnt4* in WT and *Otx2*$^{-/-}$ 6.5 dpc embryos. (*Upper*) Expression in WT embryos. (*Lower*) Expression in *Otx2*$^{-/-}$ embryos. Values at the lower right-hand corners of each picture give the abundance of the corresponding tag in either WT or *Otx2*$^{-/-}$ libraries. (Scale bar: 100 μm.)

reverse transcriptase (Life Technologies). All subsequent steps of libraries generation were performed as described by Virlon *et al.* (7) for microdissected samples.

DNA Sequencing and SAGE Data Analysis. Sequencing reactions were performed on DNA minipreps by using Big Dye terminator sequencing chemistry (Applied Biosystems) and run on 377-XL Applied Biosystems automated sequencers. Sequence files were analyzed by using SAGE software (6). Assessment of significant differences between the two libraries was made by Monte–Carlo simulation analysis (9). A P value of 0.05 or less was considered significant.

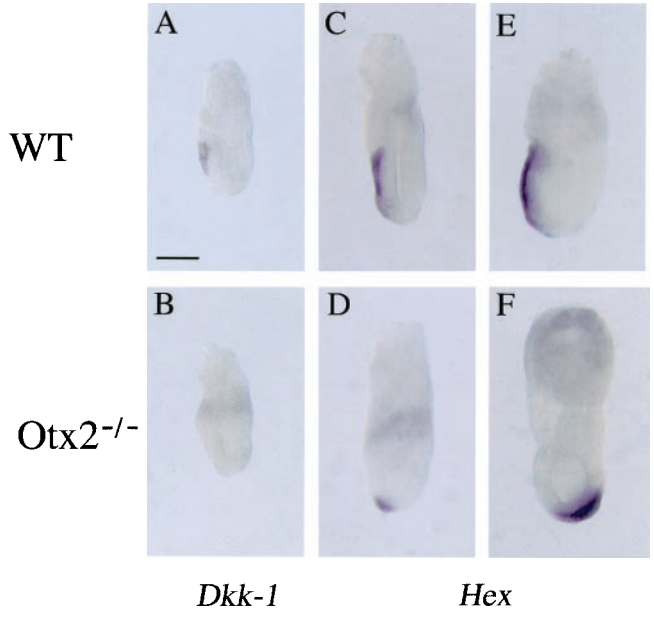

Fig. 3. Expression of mRNAs for *Dkk-1* and *Hex* in WT and *Otx2*$^{-/-}$ embryos at 6.5 and 7.5 dpc. (*A* and *B*) Expression of Dkk-1 mRNA at 6.5 dpc in WT and *Otx2*$^{-/-}$ embryos, respectively. (*C* and *D*) Expression of *Hex* mRNA at 6.5 dpc in WT and *Otx2*$^{-/-}$ embryos, respectively. (*E* and *F*) Same as *C* and *D* at 7.5 dpc. (Scale bar: 100 μm.)

Results and Discussion

Thirty embryonic portions (the extraembryonic half being used for PCR genotyping), corresponding to ≈30,000 cells, were processed for each library. A total of 27,100 and 21,443 tags were sequenced from the WT and *Otx2*$^{-/-}$ library, corresponding to 11,256 and 8,893 different tags (or transcripts), respectively. GenBank matches (known cDNAs or genes) were found for 28% of the tags from the WT library and 30% of the *Otx2*$^{-/-}$ library. The sensitivity achieved is illustrated by the fact that presence of the tags isolated from *cerberus-related-1* or *nodal* transcripts, albeit being expressed in a subpopulation of cells (10, 11) were detected by the SAGE method (Table 1).

The number of tags differentially represented ($P < 0.05$) in the two libraries, assessed by Monte–Carlo simulation, reached 141. Of those, 55 match to a cDNA (39%), 27 correspond to expressed sequenced tags (EST) (19%), and 59 are to date totally unknown (42%). A majority of these differentially represented tags correspond to genes expressed at high levels and taking part in basic cell functions not specifically related to development. Therefore, a selected set of genes was studied (Tables 2 and 3). Because genes that play important roles during embryogenesis, for instance transcription factors and secreted molecules can be poorly transcribed, tags bearing less significant variations but belonging to critical gene families were also taken into account and studied in more depth (Table 1).

To provide a potential link of these data to the *Otx2*$^{-/-}$ phenotype, whole mount *in situ* hybridization (8) was performed on WT and mutant embryos at 6.5 dpc. Six tags corresponding to genes predicted by SAGE to be differentially expressed between both types of embryos were confirmed by using this technique: (*i*) tag 123 and 15, which corresponds to an EST (331499) and to the *cystatin B* gene, respectively, and were both detected at higher levels in the mutant than in the WT library (Table 2); (*ii*) tag 187, which match to several ESTs, all highly similar to a human hypothetical protein (Q15004), and was present at a lower level in the mutant than in the WT library; (*iii*) tags corresponding to *Wnt4*, *Fgf-15*, and *eed* (*embryonic ectoderm*

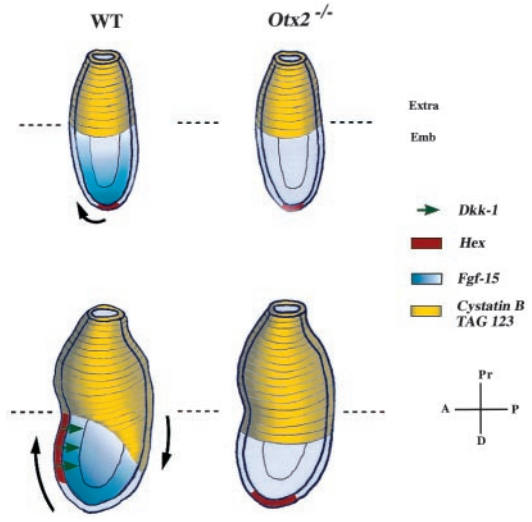

Fig. 4. Defective formation of the antero-posterior axis in early gastrulating *Otx2*$^{-/-}$ embryos. Conversion of the proximal-distal axis into the antero-posterior axis begins before gastrulation. Cells of the distal visceral endoderm undergo an oriented movement toward the future anterior pole of the embryo as illustrated by the *Hex* expression domain (shown in red). Conversely, cells of the extraembryonic endoderm expressing *cystatin B* and tag 123 appear to converge to the future posterior pole (shown in yellow). Black arrows symbolize this movement. In WT embryos, the anterior pole is also marked by the expression of *Dkk-1*. In the ectoderm layer, *Fgf-15* expression forms a gradient distributed along the proximal-distal axis before gastrulation, then along the antero-posterior axis at 6.5 dpc. In *Otx2*$^{-/-}$ embryos, the oriented movement of the cells from the visceral endoderm is abolished, resulting in the ectopic localization of the *Hex* expression domain as well as the accumulation of the *cystatin B* and tag 123-expressing cells at the embryonic–extraembryonic junction. Formation of the head organizer is also impaired, as assessed by the loss of expression of the head inductor *Dkk-1*. In addition, the ectodermal layer is affected, as shown by the absence of *Fgf-15* expression. Hence, *Otx2* is required for global cellular movements in the visceral endoderm, as well as for the proper orientation of the antero-posterior axis before gastrulation. Extra, extraembryonic region; Emb, embryonic region; A, anterior; P, posterior; Pr, proximal; D, distal. Embryos at the top are pregastrulating embryos. Embryos at the bottom are 6.5 dpc embryos.

development) mRNAs (Table 1). The mRNA known through EST 331499, which is similar to a human interferon-induced protein of unknown function (12), and that encoding the protease inhibitor *cystatin B* (13), display comparable spatial expression patterns (Fig. 1). In WT embryos, they are expressed in the extraembryonic visceral endoderm and in the embryonic posterior proximal part where the primitive streak forms (Fig. 1 *A*, *E*, and *G*). In mutant embryos, their expression domain is wider and form a ring encompassing the entire proximal embryonic region at the expense of the normal asymmetrical localization (Fig. 1 *B*, *F*, and *H*). Considering that the SAGE data were obtained from the embryonic portion, this extended distribution agrees with the fact that tags for both transcripts were much more abundant in the mutant than in the WT embryos. Fig. 1 also shows that the distribution of mRNAs for EST 331499 and *cystatin B* is strikingly complementary to the *lacZ* expression domain, which reflects sites for *Otx2* transcription. Thus, these two mRNAs locate in cells of the visceral endoderm not expressing *Otx2* and irrespective of the embryonic–extraembryonic boundary of the underlying ectoderm. Their altered distribution in mutant embryos suggests that *Otx2* is indirectly necessary for the accurate regionalization of the visceral endoderm. On the contrary, modifications in the expression profiles for tags 187, *eed*, *Wnt4*, and *Fgf-15* (Fig. 2) are associated to the embryonic ectoderm layer. Tag 187 was found in ESTs that show sequence similarity with a hypothetical human protein isolated from an immature myeloid cell line (14). The gene is expressed throughout the embryonic ectoderm (Fig. 2*A*). As expected from the SAGE data (WT count 5, *Otx2*$^{-/-}$ count 0), this expression decreases in *Otx2*$^{-/-}$ embryos without complete disappearance, suggesting that *Otx2* is necessary for its correct transcription (Fig. 2*B*). A more striking difference was found regarding *eed* transcription, which is normally ubiquitous at 6.5 dpc. *Eed* is the mouse homologue of *Drosophila extra sex combs* gene, a known repressor of homeotic genes. In mouse, it has been shown to play a role in the formation of the antero-posterior axis at gastrulation (ref. 15; Fig. 2*C*). SAGE analysis counted four times the *eed* tag in the embryonic portion of WT embryos but never in the mutants (Table 1). This result is confirmed in the *in situ* experiments in which little or no transcription is found in the embryonic region of *Otx2*$^{-/-}$ embryos (Fig. 2*D*). Conversely, *eed* expression in the extraembryonic portion is not affected. Hence, *eed* expression in the embryonic half requires presence of *Otx2*. With regards to *Fgf-15* (16), *in situ* experiments revealed that it is expressed in all embryonic ectoderm cells of WT 6.5 dpc embryos, perhaps even in a graded pattern (the cells localized at the anterior pole being more strongly stained) (Fig. 2*E*). However, no expression was detectable in mutant embryos, which agrees with our SAGE data and raises the possibility that transcription of *Fgf-15* cannot be achieved in the absence of *Otx2*. *Wnt4*, a secreted molecule involved in sexual differentiation and expressed in the developing spinal cord and kidneys (17, 18), is normally not transcribed during gastrulation. As expected, the corresponding tag could not be found in the WT library. Interestingly, its tag was counted twice in the mutant library (Table 1), and *in situ* hybridization shows a clearly distinguishable signal at the distal tip of *Otx2*$^{-/-}$ embryos (Fig. 2*H*). Thus, *Otx2*$^{-/-}$ embryos display an ectopic expression of *Wnt4* during gastrulation.

The extent of the anomalies observed in both the epiblast and visceral endoderm lead us to think that *Otx2* mutant embryos suffered global antero-posterior patterning defects. Thus, to gain deeper insights into the understanding of the *Otx2* phenotype at gastrulation, the two recently described marker genes *Dickkopf-1* (*Dkk-1*) (19) and *Hex* (20) were also tested. *Dkk-1* is a member of a family of secreted proteins and is involved in head induction. It is expressed at 6.5 dpc in the anterior visceral endoderm (AVE) (ref. 21; Fig. 3*A*) and believed to be the head organizer in mouse. *Dkk-1* transcription is abolished in the visceral endoderm of 6.5 dpc mutant embryos (Fig. 3*B*). This could account for the loss of head structures in *Otx2*$^{-/-}$ embryos. Expression of the *Hex* homeobox gene displays anterior asymmetry before gastrulation. *Hex*-expressing cells are found at the distal tip of the visceral endoderm at 5.5 dpc, and subsequently migrate to the AVE (ref. 20; Fig. 3 *C* and *E*). Our results show that, in the *Otx2*$^{-/-}$ mutant embryos, AVE precursor cells are specified. Indeed, *Hex* mRNA is expressed at the distal tip in these embryos, albeit the expected anterior migration is impeded (Fig. 2*D*). This leads, in *Otx2*$^{-/-}$ 7.5 dpc embryos, to the ectopic confinement of *Hex*-expressing cells to the region where the node is normally located (Fig. 3*F*).

Taken together, the studies of *cystatin B*, tag 123, and *Hex* expression patterns suggest that the abnormalities presented by the mutant embryos are probably because of the defective migratory properties of the visceral endoderm tissue as a whole. This may result specifically in the mislocalization of the cells fated to form the AVE, leading to an ineffective head organizer. This critical movement could perhaps be a prerequisite for the expression of the head inductor *Dkk-1*. Its absence in *Otx2*$^{-/-}$ embryos supports this hypothesis. Because it has been shown that *cerberus-related* (10) is not required for murine development, the targeted disruption of *Dkk-1* will be of great relevance for the understanding of the *Otx2* phenotype.

We also found several members of the *Wnt/β-catenin* pathway to be affected (21). For instance, mRNA levels for integrin binding protein kinase (a kinase highly homologous to human ILK) and *α-catenin* are heavily up-regulated in *Otx2* mutant embryos (Table 2). Overexpression of *ILK* could lead to the indirect depletion of *β-catenin*, by means of GSK3β (glycogen synthase kinase 3β) (22). The loss of *β-catenin* could be compensated by up-regulation of *α-catenin* because these two molecules are partially functionally redundant (23). Given the determining role of the *Wnt/β-catenin* in the formation of the Spemann organizer, it would not be surprising that *Otx2* intervenes in this signaling cascade for anterior patterning. Most interesting is the complete loss of expression of *Fgf-15* found in *Otx2* homozygous embryos. Expressed in a distal to proximal gradient in the epiblast of WT embryos, *Fgf-15* seems to parallel the expression of another secreted molecule and global regulator of antero-posterior patterning: *cripto* (24). It is worth noting that their expression domains are symmetric and complementary. *Cripto* was shown to be required for the conversion of the proximal-distal axis into the antero-posterior axis through a dialogue between the hypoblast and the epiblast. Thus, *Fgf-15* could also mediate such a function by instrumenting underlying cells of the distal endoderm to shift anteriorly. Conversely, this pattern could also reflect an *Otx2*-mediated inductive signal emanating from the visceral endoderm toward the epiblast (Fig. 4). A similar hypothesis can be suggested for the mRNA corresponding to tag 187 (Q15004), which is much more expressed in WT than in $Otx2^{-/-}$ embryos in the embryonic ectoderm. Deciphering the function of this mRNA, as well as identification of the *Fgf-15* partners, could lead to a deeper molecular understanding of neural induction and morphogenetic movements during gastrulation. Nevertheless, it becomes more and more apparent that *Otx2* plays a pivotal role in very early development, perhaps as soon as 5.5 dpc or earlier in the global control of antero-posterior patterning through modulation of morphogenetic movements. It is noteworthy that the inactivation of *Otx2* entails the double knockouts of *Dkk-1* and *Fgf-15* in the visceral endoderm and epiblast, respectively, in gastrulating mouse embryos.

In conclusion, the application of SAGE to the understanding of the *Otx2* phenotype at gastrulation delivered extensive information. It allowed to identify transcripts whose regulation is modified in the absence of the *Otx2* protein. Because SAGE provides such considerable amounts of data, a systematic functional screening needs to be set up to readily have access to the tags of primary interest. In the near future, confrontation of independent SAGE libraries performed at the same embryonic stage but over distinct mutations will permit the unraveling of genetic cascades and a better discernment on the direct effects of each mutation.

We thank Dr. J. C. Aude for updating the SADE web site with mouse embryos data. This work was supported by grants from the European commission Biotech CT-96-0378, the Association Francaise contre les Myopathies, and the Centre National de la Recherche Scientifique.

1. Cohen, S. & Jurgens, G. (1990) *Nature (London)* **346,** 482–485.
2. Klein, W. H. & Li, X. (1999) *Biochem. Biophys. Res. Commun.* **258,** 229–233.
3. Simeone, A., Acampora, D., Gulisano, M., Stornaiuolo, A. & Boncinelli, E. (1992) *Nature (London)* **358,** 687–690.
4. Acampora, D., Mazan, S., Lallemand, Y., Avantaggiato, V., Maury, M., Simeone, A. & Brûlet, P. (1995) *Development (Cambridge, U.K.)* **121,** 3279–3290.
5. Rhinn, M., Dierich, A., Shawlot, W., Behringer, R. R., Le Meur, M. & Ang, S.-L. (1998) *Development (Cambridge, U.K.)* **125,** 845–856.
6. Velculescu, V., Zhang, L., Vogelstein, B. & Kinzler, K. (1995) *Science* **270,** 484–487.
7. Virlon, B., Cheval, L., Buhler, J.-M., Billon, E., Doucet, A. & Elalouf, J.-M. (1999) *Proc. Natl. Acad. Sci. USA* **96,** 15286–15291.
8. Henrique, D., Adam, J., Myat, A., Chitnis, A., Lewis, J. & Ish-Horowicz, D. (1995) *Nature (London)* **375,** 787–790.
9. Zhang, L., Zhou, W., Velculescu, V. E., Kern, S. E., Hruban, R. H., Hamilton, S. R., Vogelstein, B. & Kinzler, K. W. (1997) *Science* **276,** 1268–1272.
10. Belo, J. A., Bouwmeester, T., Leyns, L., Kertesz, N., Gallo, M., Follettie, M. & De Robertis, E. M. (1997) *Mech. Dev.* **68,** 45–57.
11. Varlet, I., Collignon, J., Robertson, E. (1997) *Development (Cambridge, U.K.)* **124,** 1033–1044.
12. Pennacchio, L. A. & Myers, R. M. (1996) *Genome Res.* **6,** 1103–1109.
13. Luster, A., Weinshank, R., Feinman, R. & Ravetch, J. (1998) *J. Biol. Chem.* **263,** 12036–12043.
14. Nagase, T., Seki, N., Tanaka, A., Ishikawa, K. & Nomura, N. (1995) *DNA Res.* **2,** 199–210.
15. Shumacher, A., Faust, C. & Magnuson, T. (1996) *Nature (London)* **383,** 250–253.
16. McWhirter, J., Goulding, M., Weiner, J., Chun, J. & Murre, C. (1997) *Development (Cambridge, U.K.)* **124,** 3221–3232.
17. Stark, K., Vainio, S., Vassileva, G. & McMahon, A. P. (1994) *Nature (London)* **372,** 679–683.
18. Vainio, S., Heikkila, M., Kispert, A., Chin, N. & McMahon, A. (1999) *Nature (London)* **397,** 405–409.
19. Glinka, A., Wu, W., Delius, H., Monaghan, A. P., Blumenstock, C. & Niehrs, C. (1998) *Nature (London)* **391,** 357–362.
20. Thomas, P. Q., Brown, A. & Beddington, R. (1998) *Development (Cambridge, U.K.)* **125,** 85–94.
21. Moon, R. & Kimelman, D. (1998) *BioEssays* **20,** 536–545.
22. Novak, A., Hsu, S.-C., Leung-Hagesteijn, C., Raveda, G., Papkoff, J., Montesano, R., Roskelley, C., Grosschedl, R. & Dedhar, S. (1998) *Proc. Natl. Acad. Sci. USA* **95,** 4374–4379.
23. Vleminckx, K. & Kemler, R. (1999) *BioEssays* **21,** 211–220.
24. Ding, J., Yang, L., Yan, Y.-T., Chen, A., Desai, N., Wynshaw-Boris, A. & Shen, M. M. (1998) *Nature (London)* **395,** 702–707.